

# DESIGN OF FFA MAGNET FOR THE LASER-HYBRID ACCELERATOR FOR RADIOBIOLOGICAL APPLICATIONS (LhARA)

T.J.Kuo\*, J. Pasternak, Imperial College London, UK  
J.-B. Lagrange, STFC/RAL, UK

## Abstract

LhARA, which stands for “Laser-hybrid Accelerator for Radiobiological Applications”, is a novel and flexible facility dedicated to research in radiobiology. A proton beam of energy up to 15 MeV can be produced by a laser driven source, the beam then enters a Fixed Field Alternating (FFA) gradient accelerator for acceleration to produce a variable extraction energy between 15-127 MeV. To avoid uncontrolled beam loss, the operational tune was picked carefully to avoid resonances. The magnetic field must be adjusted to ensure that the tune stays at the same working point for different energy ranges. The FFA ring uses combined-function spiral magnets, which create a radial magnetic gradient through distributed conductors wrapped around the pole, each carrying a different current. A three-dimensional study was carried out in OPERA 3D and the parameters of the magnet were optimized. The results showed that resonances up to fourth order were avoided for the entire range of acceleration for different operational energies.

## INTRODUCTION

The Laser-hybrid Accelerator for Radiobiological Applications (LhARA) is an innovative and versatile facility designed specifically for radiobiology research [1]. It produces a proton beam through laser-driven interactions, which is then captured by a Gabor lens [2]. The facility's design includes two stages: a proton beam up to 15 MeV can directly enter a low-energy in-vitro end station or be redirected through an injection line into a Fixed Field Alternating (FFA) gradient accelerator for further acceleration. A more detailed description of the whole facility can be found in [3]. The use of fixed field magnets means that acceleration can proceed as rapidly as the RF cavities permit. The FFA also supports variable extraction energy; proton beams from 15 MeV to 127 MeV can be produced. The ability to produce variable energy, high repetition rate, and ultra short beams allows LhARA to investigate a wide spectrum of radiobiological effects. In order to avoid beam loss, the magnets must meet the following requirements:

- Zero chromaticity during acceleration (constant tune)
- Constant working tune point for different energy ranges
- Sufficient physical and dynamical apertures

## MAGNET SPECIFICATIONS

The FFA ring is composed of ten identical cells; each featuring a single combined-function spiral magnet with

\* tk1218@ic.ac.uk

nonlinear magnetic gradient radially providing focusing in the transverse plane. The entrance and exit faces of the magnet form a spiral from the machine centre, creating a non perpendicular angle between the magnetic pole and the orbits. This provides additional focusing and defocusing actions through edge focusing; therefore strong focusing is realized without a reverse bending magnet, minimizing the circumference of the machine.

The magnetic field profile is achieved through a combination of distributed conductors: a main coil, and 18 trim coils. The main coil, wound around the pole, produces a uniform dipole field. The trim coils cross the pole face and return toward the pole's outer radius as shown in Fig. 1; they are individually powered to generate the necessary field gradient. The trim coil returns are designed to maximize power efficiency, with their magnetic fields contributing constructively to the main dipole field. To minimize field errors, the trim coils are arranged in two overlapping layers on the pole face. This configuration has been shown to reduce magnetic field errors by a factor of five compared to a non-overlapping arrangement [4]. The current settings can be adjusted to accommodate different energy ranges while maintaining the same field index  $k$  in order to be at the same working tune point.

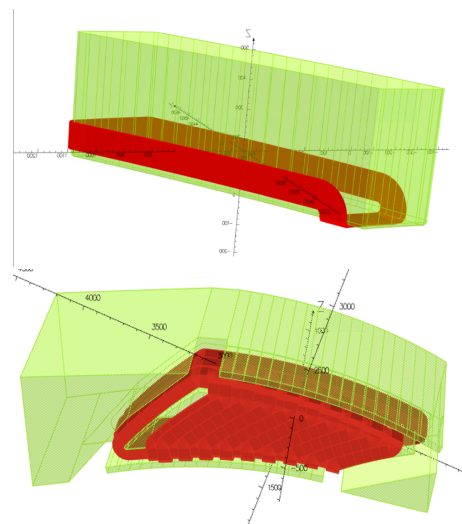


Figure 1: (Top) Opera-3D model showing a piece of trim coil wrapped around the pole. The trim coil crosses the pole face and returns around the side of the pole. (Bottom) Upper half of the magnet with all the coils. The centre of the machine is towards the right of the image

The LhARA FFA magnet is an H-type magnet with 50 mm thick clamps added on either side all connected via a com-

mon iron yoke. This configuration was found to better contain the fringe fields than having separate clamps. The parameters of the magnet are listed in Table 1.

Table 1: Parameters of the magnet

Cell type	Spiral
k value	5.23
spiral angle (deg)	53.9
Magnet opening angle (deg)	12.24
Full gap size (mm)	96
Minimum radius of the pole (mm)	2770
Minimum orbit excursion (mm)	2880
Maximum radius of the pole (mm)	3740
Maximum orbit excursion (mm)	3530
Target horizontal ring tune	2.79
Target Vertical ring tune	1.17

## PROCEDURE

A constant tune can be achieved using non-scaling magnets [5], but scaling magnets offers operational simplicity. Optimizing the magnet for a single energy level naturally extends across the entire acceleration range. This is especially beneficial for variable energy extraction, where uniform behavior across different energy ranges is essential. The goal is to ensure that the integrated magnetic field  $BL$  along the midplane adheres to the scaling law:

$$BL = BL_0 \left( \frac{r}{r_0} \right)^{k+1} \quad (1)$$

where  $r_0$  is the reference radius chosen and  $BL_0$  the integrated magnetic field at that radius.

The integrated field  $BL$  is defined as:

$$BL(r) = \int B(r, \theta) r d\theta \quad (2)$$

where  $r$  and  $\theta$  are cylindrical coordinates. An example of how  $B(r, \theta)$  varies with  $r$  and  $\theta$  is shown in Fig. 2.

The field index  $k$  is defined as:

$$k(r) = \frac{r}{BL(r)} \frac{\partial BL(r)}{\partial r} - 1 \quad (3)$$

Both the field index  $k$  and the spiral angles  $\zeta$  of the field should be kept as constant as possible. The spiral angles are calculated using the angle of the centre of moment,  $\theta_{COM}$  on the longitudinal gradient of the field along a constant radius.

$$\theta(r)_{COM_{En,Ex}} = \frac{\int \frac{\partial B(r, \theta)}{\partial \theta} \theta d\theta}{\int \frac{\partial B(r, \theta)}{\partial \theta} d\theta} \Big|_{\frac{\partial B(r, \theta)}{\partial \theta} < 0, \frac{\partial B(r, \theta)}{\partial \theta} > 0} \quad (4)$$

The sign of edge focusing at the boundaries of the magnet are opposite; defocusing and focusing in the horizontal plane for the entrance (En) and exit (Ex) side of the magnet

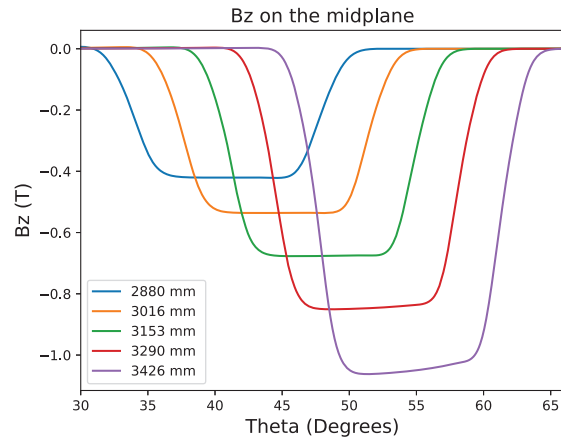


Figure 2: Azimuthal field profile at different radius on the midplane for the highest extraction energy case (127 MeV). At higher radii the flat top of the field is distorted due to saturation effects.

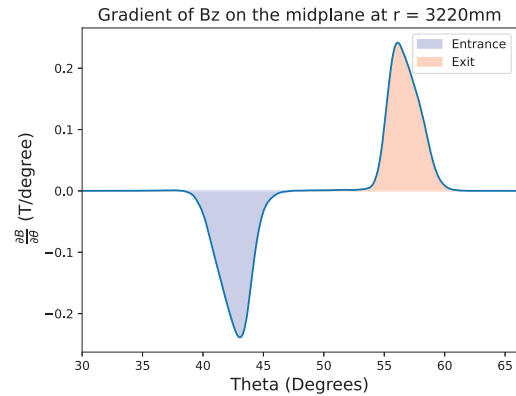


Figure 3: Azimuthal field gradient at a constant radius on the midplane. Using where the gradient crosses zero as a boundary, the integrals can be split into two sections: entrance and exit of the magnet

respectively.  $\theta_{COM}$  is calculated separately with boundaries shown in Fig. 3.

The spiral angles can then be calculated as:

$$(r)_{En,Ex} = \arctan \left( r \frac{\partial \theta(r)_{COM_{En,Ex}}}{\partial r} \right) \quad (5)$$

## RESULTS

Two different energy ranges were investigated. The maximum energy case: 15 MeV injection energy accelerated to 127 MeV and a lower energy case: 7 MeV injection energy accelerated to 57 MeV. After optimization, the final values of the  $k$  index and spiral angles  $\zeta$  were calculated and shown in Fig. 4 and Fig. 5 respectively. The oscillations in the results are due to the discretizations of the trim coils, the amplitude of the oscillations cannot be decreased by further optimiz-

ing the current settings. 3D field maps were obtained and tracked in Fixfield [6], the ring tunes were plotted against resonances up to fourth order as shown in Fig. 6.

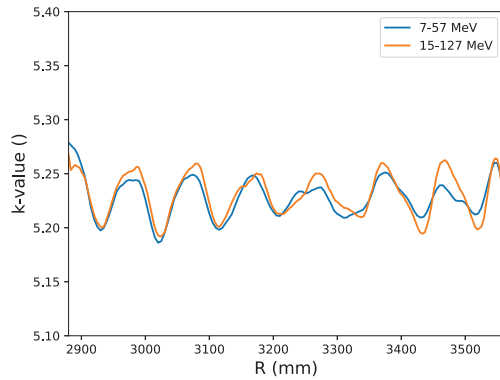


Figure 4: Field index  $k$  of the magnet for two different energy ranges.

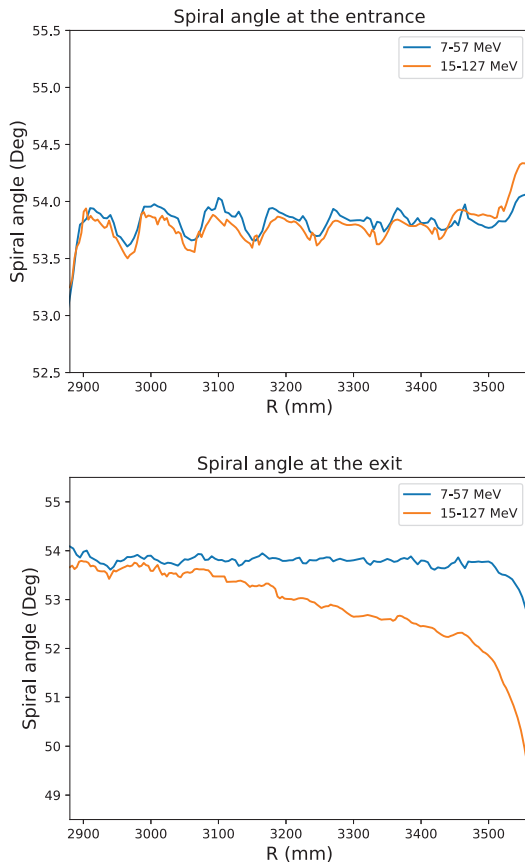


Figure 5: Spiral angles of the magnet. The exit spiral angle decreases at large radii due to saturation effects.

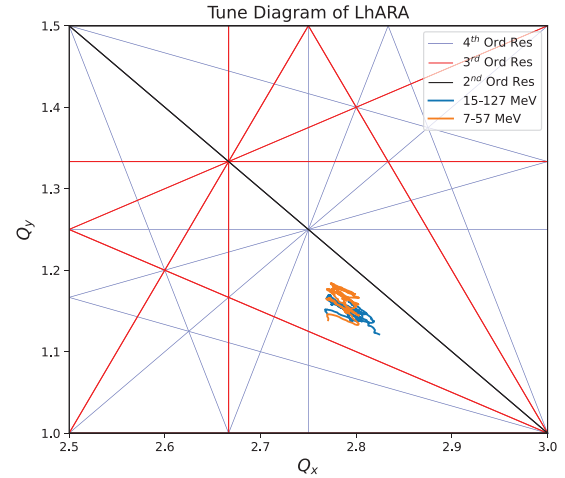


Figure 6: Ring tune variation of two energy ranges. The working tune points overlap and avoid any resonances up to the fourth order.

## CONCLUSION

To demonstrate the ability to produce variable extraction energies, two separate energy ranges with 57 MeV and 127 MeV extraction energy respectively were investigated. The current settings have been optimized to keep the integrated fields as close to the scaling condition as possible with the same field value  $k$ ; while scaling  $BL_0$  to accommodate different energy ranges. The ring tune variation of the LhARA FFA is already shown to be small enough to avoid resonances up to fourth order for the energy ranges stated above.

Further work will be done on reducing the fringe field extent variation to further reduce the tune spread, allowing a greater margin of error. The performance of the ring will also be confirmed for the full extraction energy range (15-127 MeV). Finally, a study at different energy ranges is needed to check that the dynamic aperture is sufficient for machine operation.

## REFERENCES

- [1] G. Aymar, *et al.*, “LhARA: The Laser-hybrid Accelerator for Radiobiological Applications”, *Front. Phys.*, vol. 8, Sep. 2020. doi: 10.3389/fphy.2020.567738
- [2] D. Gabor, “A Space-Charge Lens for the Focusing of Ion Beams”, *Nature*, vol. 160, pp. 89-90, 1947. doi: 10.1038/160089b0
- [3] W. Shields, *et al.*, “Status update of the laser-hybrid accelerator for radiobiological applications”, presented at IPAC’25, Taipei, Taiwan, Jun. 2025, paper TUPB103, this conference.
- [4] I. Rodriguez, *et al.*, “FFA magnet prototype for high intensity pulsed proton driver”, in *Proc. IPAC’23*, Venice, Italy, May 2023, pp. 2261–2264. doi: 10.18429/JACoW-IPAC2023-TUPM032

- [5] S. Brooks, “Non-scaling fixed-field proton accelerator with constant tunes”, in *Proc. IPAC’23*, Venice, Italy, May 2023, pp. 2257–2260.  
doi:10.18429/JACoW-IPAC2023-TUPM031
- [6] J.-B. Lagrange, “The Particle Tracking Code Fixfield”, in *Proc. IPAC’21*, Campinas, Brazil, May 2021, pp. 1905–1906.  
doi:10.18429/JACoW-IPAC2021-TUPAB209